

Lateral diffusion in tethered bilayer membranes

Master Thesis

Mathieu Jung

Max Planck Institute for Polymer Research
Mainz, Germany

-

Martin-Luther University
Halle (Saale), Germany

October 2005

Summary:

I.	Introduction:.....	1
II.	Materials and Methods:.....	4
A.	Tether Molecules:	4
1.	The anchor group:	5
2.	The tethered spacer:	6
3.	The hydrophobic chains:.....	6
B.	Lipids:	7
1.	1,2-diphytanoyl-sn-glycero-3-phosphoethanolamine (DPhyPE).....	7
2.	N-(7-nitrobenz-2-oxa-1,3-diazol-4-yl)-1,2-dihexadecanoyl-sn-glycero-3-phosphoethanolamine ammonium salt (NBD-PE).....	8
C.	SiO _x Supports:	9
D.	Langmuir – Blodgett – Kuhn (LBK) Film Transfer:	10
1.	Physical Principles:	10
2.	Surface pressure – area isotherms:.....	11
3.	Film deposition:	12
E.	Bilayer formation:	13
F.	Contact angles:.....	13
G.	Fluorescence recovery after photobleaching (FRAP).....	15
1.	Measurement procedure and evaluation:	16
2.	Diffusion in homogeneous systems:	17
III.	Results and discussion:	19
A.	Langmuir Isotherms:	19
B.	Optical fluorescence microscopy:.....	23
C.	DPTTE or DPTTM? :	25
D.	FRAP Measurements:	28
1.	Inner leaflet:	28
2.	Outer leaflet:	30
IV.	Conclusion:	32
V.	Literature:.....	34
	Acknowledgments:	36

I. Introduction:

Cell membranes are one of the essential structural and functional elements of living organisms. Most fundamentally, the plasma membrane of a cell denotes the outer boundary of it and distinguishes between the “inside” and the “outside”. However, this barrier has to be selectively permeable to permit exchange of nutriments and wastes between the two worlds. Simultaneously, the biomembranes developed into sites of essential biochemical functions, such as signal transduction or protein biosynthesis. This implies the establishment of transmembrane gradients of solutes, pH or electrical charges.

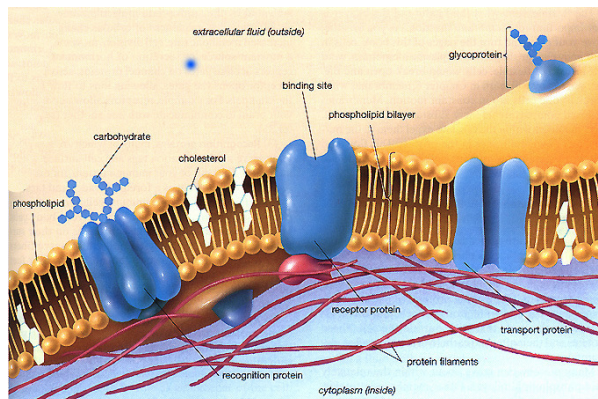


Fig 1: Taken from *Human Biology* by Daniel Chiras

Biological membranes consist of a quasi two-dimensional macromolecular assembly of amphiphilic lipids and proteins, supported by rigid biopolymer layers, e.g. a cytoskeleton or a glycocalyx matrix, providing mechanical stability.

The understanding and governing of this unique support is of crucial importance for the study and, in the near future, the controlled use of proteins.

Therefore several model membranes were developed in the past decade to study the physical properties of biological membranes. Some of them are schematically shown in Fig 2.

The first and most widely used one is the vesicle. Vesicles are spherical lipid bilayers [1]. They are easy to produce at a defined size. On the other hand, this system has a short lifetime and needs to be fixed with special apparatus to be used in measurements describing the transmembrane actions of the proteins.

A second model system, the so-called black lipid membranes (BLM), consists of a lipid bilayer that is spanned over a small pinhole [2, 3]. Its high electrical sealing properties due to the compact arrangement of the lipids makes them very interesting for bilayer studies. But they suffer the disadvantage to be delicate to produce and mechanically highly unstable.

The direct deposition of lipid bilayers onto solid substrates leads to solid-supported lipid bilayers (SSM) [4]. SSM's can be used to investigate proteins attached to the outer leaflet of the bilayer membrane, such as annexin [5]. Due to their lack of space beneath the membrane, they are not suitable for proteins having external domains and requesting an ionic reservoir beneath the bilayer.

The last improvement in the field of model membranes was achieved by the separation of the bilayer from the support using low molecular weight hydrophilic spacers. These spacer groups provide the possibility to build an aqueous reservoir between the lipid bilayer and the substrate. At the same time the bilayer is covalently tethered to the surface. The membranes are therefore referred to as tethered bilayer lipid membranes (tBLMs) [6-9]. These tBLMs combine the advantage of being very stable due to the support and permitting the exploration of proteins having external domains and ion transport across the bilayer.

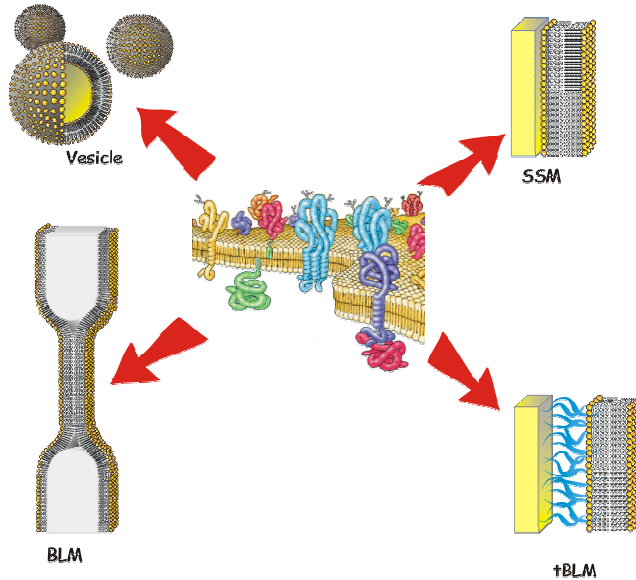


Fig 2: Model systems for biological membranes.

Our research group has focused on tBLMs in order to study the mechanism of membrane proteins and to use them as a sensing element in biosensor applications. For this purpose different types of spacer molecules, based on oligoethyleneglycol moieties for the hydrophilic part and diphthanyl groups for the hydrophobic part, have been synthesized. More details about these molecules will be provided further on.

The crucial point of this development is to achieve a densely packed bilayer on the substrate to ensure low leakage currents through the membrane. The supports of interest are noble metals or doped silicon oxide suiting the needs of the biosensor industry. By use of a conductive support, electrochemical characterisation of the membrane is feasible. This also gives rise to an electrochemical-sensing platform allowing the registration of the electrical potentials induced by the active protein. Furthermore, it is also possible to apply a whole range of surface analytical techniques such as atomic force microscopy, ellipsometry, surface plasmon resonance, etc, to characterize the membranes.

Within the macromolecular aggregation of a biological membrane, lipids and proteins retain their association with each other without the benefit of covalent bonds. While the individual components, the membrane proteins and the membrane lipids are constituted of covalent bonds, their association with each other to produce specific membrane structures is governed largely by the hydrophobic effect. The ensemble membrane – protein is built up in such a way that the bilayer is first formed and the proteins are introduced afterwards. Therefore lateral mobility of the lipids inside the membrane is of crucial importance for the successful incorporation of large membrane protein complexes. Additionally, fluidity in the membrane is also necessary to allow for a proper function of the proteins.

Resulting from these observations, the aim of this work was to study to which extend the tethering of our model membrane to the support hinders the movement inside both leaflets and furthermore impedes the incorporation of proteins. **Fluorescence Recovery After Photobleaching (FRAP)** was applied to investigate this question. This method is based on the measurement of chromophores diffusing from a fluorescent surface into a non-fluorescent spot.

II. Materials and Methods:

A. Tether Molecules:

The tBLMs we investigated were based on two molecules:

- 2,3-di-O-phythanyl-sn-glycerol-1-tetra-ethylene glycol-(3-triethoxy-silane) ether lipid (DPTTE)
 - 2,3-di-O-phythanyl-sn-glycerol-1-tetra-ethylene glycol-(3-trimethoxy-silane) ether lipid (DPTTM)

The chemical formulas are depicted below.

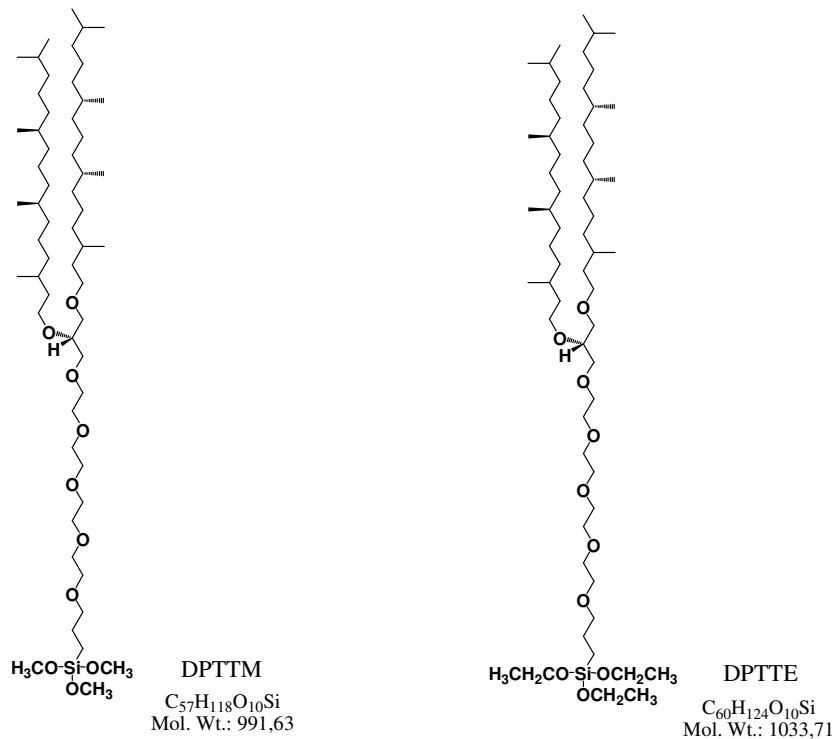


Fig 3: Chemical formulas of the tether lipids used in this study.

These molecules can be seen as the assembly of three components, playing each a specific role in the membrane: the anchor, the spacer, and the chains [10].

1. The anchor group:

Anchor groups based on silane derivatives are used to immobilize lipopolymers on silicon oxide supports. The coating of the support with the inner leaflet of the membrane is achieved via Langmuir-Blodgett-Kuhn Film Transfer (LBK), which is discussed in chapter II.D.

It is assumed that the grafting mechanism of the trialkoxysilane groups is composed of three different phases:

- 1) The trialkoxysilane groups are first hydrolysed in the water subphase.
- 2) By use of LBK transfer the lipid film is deposited on the support, where the hydroxysilanes are bound via hydrogen bonds to the hydroxy-groups present on the substrate.
- 3) By removal of water molecules condensation reaction takes place, leading to a network in which each lipid is linked to the surface and possibly to the neighbours.

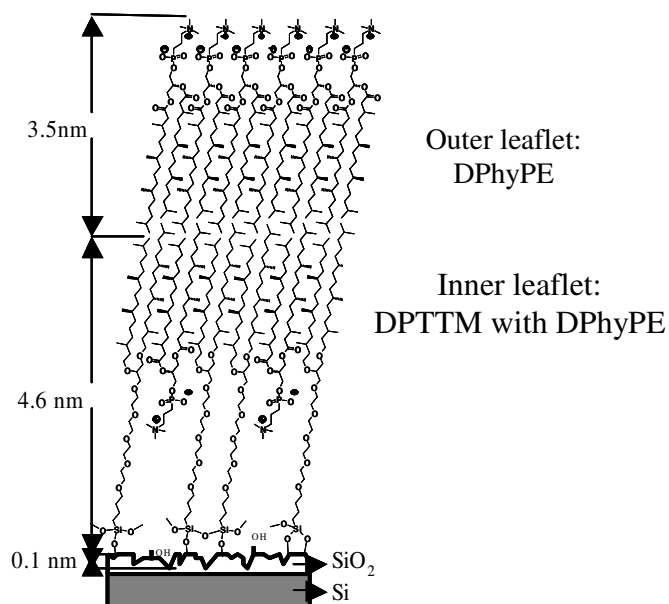


Fig 4: Schematic representation of the arrangement of the DPTTM molecules and DPhyPE (1,2-diphytanoyl-sn-glycero-3-phosphoethanolamine) forming a tBLM.

2. The tethered spacer:

The appropriate choice of the spacer unit is decisive. It has to fulfill the following conditions:

- Hydrophilic to encourage the creation of an ion reservoir between membrane and support
- Physically inert to prevent adsorption on the substrate
- Chemically inert to prevent interactions either with membrane lipids or proteins

To suit these requirements, oligo(ethylene glycol) chains are optimal candidates.

Parallel to tetra(ethylene glycol) spacers, lipopolymers with hexa-, octa-, dodeca- and tetradeca(ethylene glycol) units were synthesized. The idea is to customize the ion reservoir to the needs of the embedded protein. However, in this study we used only tetra spacers, already used for membranes showing functional incorporation of valinomycin and gramicidin D [10].

3. The hydrophobic chains:

As hydrophobic part, two phytanoyl chains are fixed to the spacer by means of ether linkage. Other research groups described the use of ester bridges to link the two parts, but these suffer the disadvantage to easily undergo hydrolytic cleavage, whereas ether bridges are more stable [11, 12].

Furthermore, it is known that lipids with low phase transition temperatures have short acyl chains (e.g. caproyl-, lauroyl-chains) or cannot pack properly due to double bonds or side chains (e.g. oleoyl-, phytanoyl-chains). In opposition, lipids with long, saturated alkyl chains (e.g. palmitoyl-chains) have a high phase transition temperature [13].

To prevent phase separation between lipopolymer and lipids, hydrophilic tails with side chains that have a solid-liquid phase transition under room temperature were preferred.

B. Lipids:

1. 1,2-diphytanoyl-sn-glycero-3-phosphoethanolamine (DPhyPE)

The inner leaflet of our membranes was assembled with mixtures of lipopolymer / lipids at different ratios, with the aim to improve its fluidity.

The lipid of our choice was DPhyPE because of its high analogy to the DPTTM (and DPTTE) mainly due to the presence of the two phytanoyl chains.

Inserted in the membrane, DPhyPE and DPhyPC (1,2-diphytanoyl-sn-glycero-3-phosphocholine) molecules require more space at the tails than the head (due to the methyl-side chains). Moreover, at room temperature they are found to be in fluid phase, but showing a defined arrangement of the hydrophobic chains [14-18].

These properties induce a very low permeability of the membrane to ions and stabilize the lipid bilayer. Therefore these lipids are also very often used to build membranes in order to perform experiments on channel proteins.

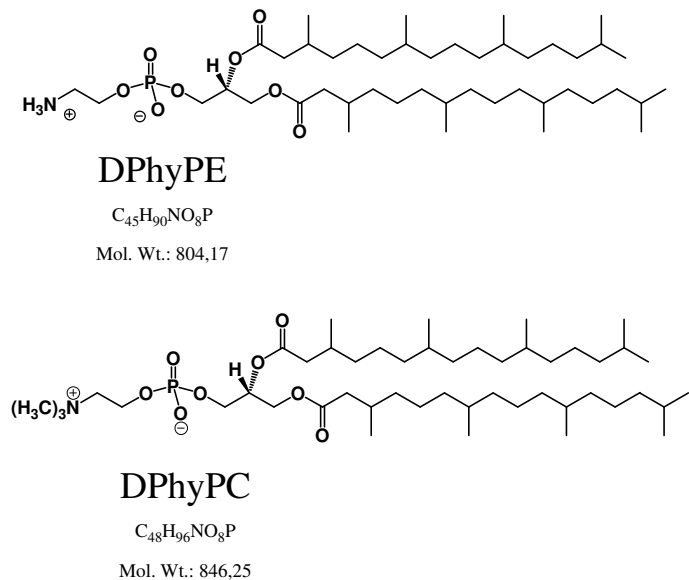


Fig 5: Chemical structures of DPhyPE and DPhyPC

2. N-(7-nitrobenz-2-oxa-1,3-diazol-4-yl)-1,2-dihexadecanoyl-sn-glycero-3-phosphoethanolamine ammonium salt (NBD-PE)

In order to perform FRAP experiments an adequate fluorescent marker is needed. On one side it has to be easily and irreversibly bleachable at high light intensity and on the other side have a high fluorescence even at low light excitation. NBD-PE suits these requirements. The chemical structure is shown in Fig 6.

Furthermore we chose NBD-PE because of its similar structure to DPhyPE, which makes it easy to incorporate in the membrane. The fluorescent group NBD needs very little space and therefore does not disturb the lipid structure at low concentrations.

Through all experiments, we kept a constant NBD-PE concentration of 0.8 mol%.

The absorption maximum of NBD-PE is at 463 nm with an emission maximum at 536 nm, as can be seen in Fig 7.

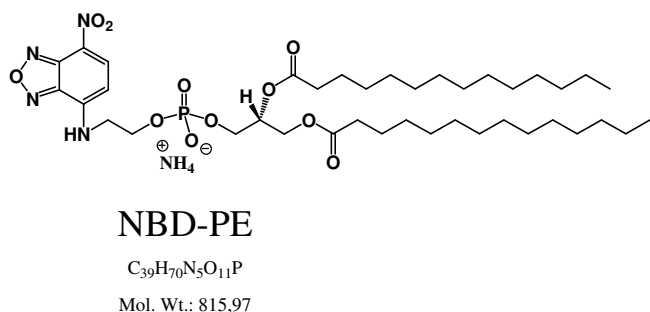


Fig 6: Chemical structure of NBD-PE

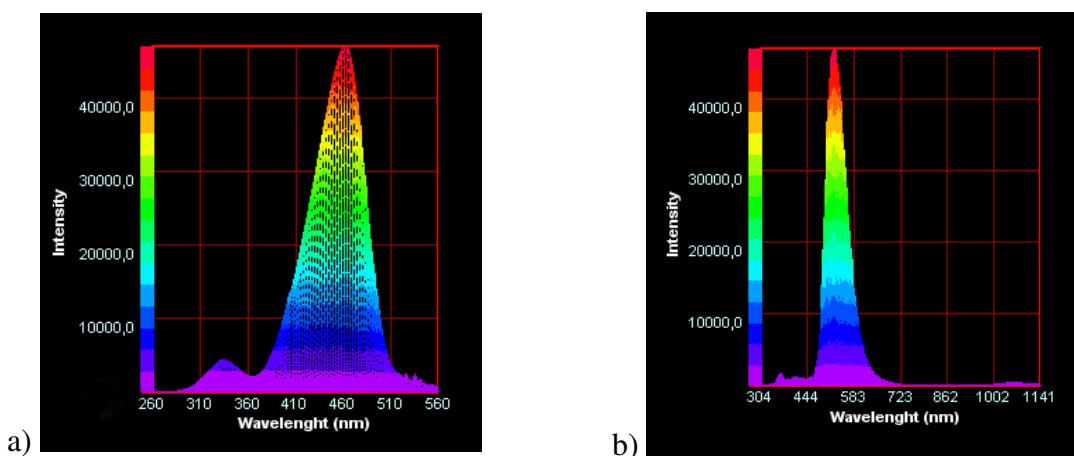


Fig 7: Excitation spectra (a) and emission spectra (b) (at 460 nm) of NBD-PE.

All lipids were purchased from Avanti Polar Lipids, Alabaster U.S.A, and used without further purifications.

C. SiOx Supports:

Fig 4 shows the membrane height to be approx. 8 nm in completely stretched form. In addition, a perfectly planar membrane hinders the formation of defects and so promotes its electrical sealing properties.

The roughness and cleanliness of the substrate is of highest importance, therefore we used polished silicon wafers as support (2cm x 2cm) that first had to go through various preparation and cleaning procedures. Silicon wafers with 100-110 nm thermal oxide were obtained from S. Ingebrandt, research Centre Jülich, Germany.

Furthermore, to eliminate all residues sticking at the surface we pursue following cleaning procedure:

- 10 min. ultrasonic bath in ethanol (HPLC grade)
- 10 min. ultrasonic bath in a 2% Hellmanex solution, from Hellma, Müllheim, Germany (alkaline liquid for cleaning quartz, glass or sensitive optical components)
- 10 min. ultrasonic bath in pure water (MilliQ, with $R > 18\text{M}\Omega\text{cm}$)
- 1 hour at 75°C in a solution of 5 parts MilliQ – 1 part H_2O_2 (30%vol) – 1 part ammonia (30%)
- Intensive rinsing with MilliQ
- 5 min. 300W plasma cleaning (0.9mbar argon/0.1mbar oxygen)

This procedure increases the surface coverage of OH-groups on the surface.

D. Langmuir – Blodgett – Kuhn (LBK) Film Transfer:

The proximal leaflet of the membranes can be deposited on a solid substrate by different techniques, e.g. self-assembly or Langmuir – Blodgett – Kuhn technique. We want to control precisely the lateral density of the lipopolymer/lipid mixture on the surface. The LBK technique offers the possibility to transfer pre-defined mixtures in a controlled manner, leading to homogeneous surface monolayers [19-24].

The LBK films were prepared on a KSV Mini-Trough from KSV Instruments Ltd, as schematically depicted in Fig 8. It is composed of a Teflon trough, containing the water subphase in which the support is immersed. Movable Teflon barriers at both sides of the trough permit the control of the spreading area. Finally, a Wilhelmy plate measures the surface pressure.

1. Physical Principles:

Amphiphiles spread instantaneously when applied to the air/water interface and form monolayers, as the solvent evaporates. When the area available for the monolayer is large, the distance between adjacent molecules is large and their interactions are weak. In this case, the monolayer can be regarded as a two-dimensional gas; the monolayer has little effect on the water surface tension. If the available surface area is reduced by a barrier system, the molecules start to exert a repulsive effect on each other. This two-dimensional analogue of a pressure is called surface pressure, π and is given by the following relationship:

$$\pi = \gamma_0 - \gamma$$

Eq.1

where γ_0 is the surface tension in absence of a monolayer and γ the surface tension in presence of the monolayer. The surface pressure can be measured by the Wilhelmy plate-method. The forces resulting from the surface tension are measured on a partially immersed platinum plate. These forces are then converted into surface pressure (mN/m) with the help of the plate dimensions.

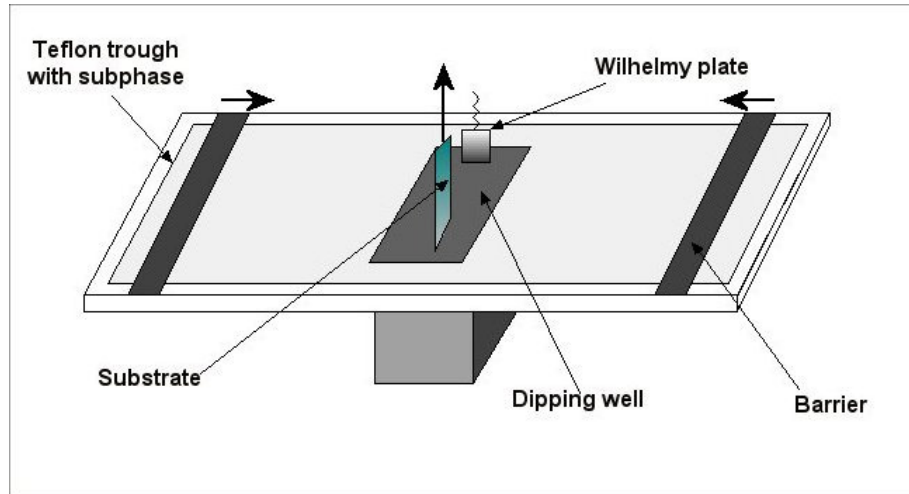


Fig 8: Schematic drawing of a Langmuir – Blodgett – Kuhn film transfer apparatus.

2. Surface pressure – area isotherms:

By spreading a defined amount of amphiphilic molecules on the air-water interface, it is possible to determine the mean molecular area (A), i.e. the mean space occupied by each molecule. A surface pressure/area isotherm is measured by moving the barriers to compress the film and simultaneous recording of the change in the surface pressure.

Since π is the derivative of the surface free energy with respect to the intrinsic variable A , it is a thermodynamic variable. Therefore changes in the slope of the π - A isotherms at constant temperature can be used to identify and characterize phase transitions[25].

A typical isotherm for phospholipids is given in Fig 9.

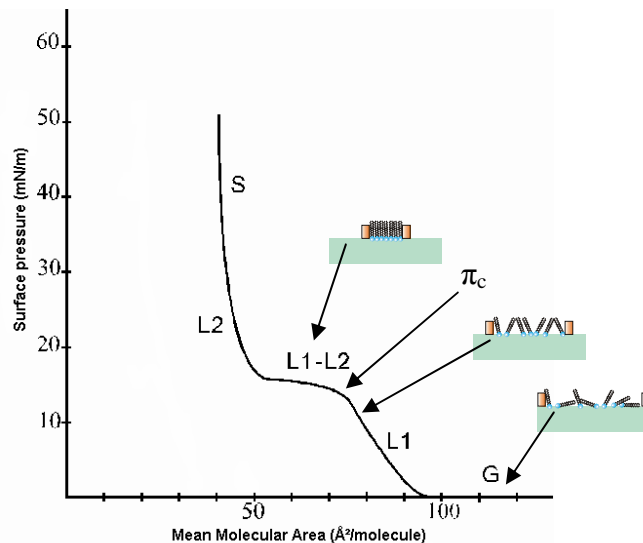


Fig 9: Typical π - A isotherm of phospholipids with schematic ordering of the lipids. Indicated is the point π_c as the main phase transition.

One can distinguish five different phases, characterized by a change in the slope of the isotherm.

- G: the gas phase, the interactions between the molecules are too weak to be noticed,
- L1: the liquid expanded state,
- L1-L2: transition plateau,
- L2: the liquid ordered state,
- S: the solid state.

After reaching the solid state, the film usually collapses into tree-dimensional structures.

3. Film deposition:

Once the film surface is compressed to the desired surface pressure (30mN/m) or molecular area, the previously immersed SiO_x support can be withdrawn from the aqueous subphase at constant rate (7mm/min), entraining at the same time the created film on its surface.

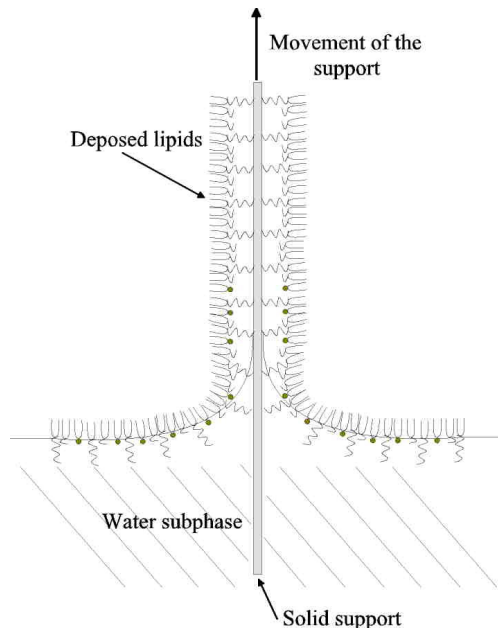


Fig 10: Schematic representation of the film transfer procedure (the green dots stand for the fluorescent marker).

Simultaneously, the barriers keep the surface pressure constant, by closing accordingly to the Wilhelmy-plate response.

The films were allowed to dry overnight in a desiccator, and afterwards baked at 50°C for 40 min. For our purposes, films were transferred at the higher end of the liquid expanded state.

E. Bilayer formation:

In this study, the proximal leaflets of the membranes were always assembled using the LBK technique.

In order to grow bilayers on top of these layers, different methods are suitable; the two prominent ones are Langmuir-Schäfer transfer and vesicle fusion. We chose the second way in order to be able to compare results to previous experiments [26].

Vesicles of 50nm diameter were produced by extrusion of a 0.2mM DPhyPE solution in MilliQ, containing 0.8mol% NBD-PE. These vesicles were added to the monolayer, immersed in buffer solution (20 μ l vesicles/1ml buffer), typically 100mM NaCl. As shown elsewhere bilayer growth is completed after 5-6 hours.

F. Contact angles:

Contact angle measurements are a rapid and effective method to evaluate the quality of the deposited film. The contact angle θ , formed by a liquid on a surface at the three phase boundary where liquid, solid and gas intersect, is a quantitative measure of the hydrophilicity of a surface.

It can also be considered in terms of the thermodynamics of the materials involved. This analysis involves the interfacial free energies between the three phases and is given by:

$$\gamma_{lv} \cos \theta = \gamma_{sv} - \gamma_{sl}$$

Eq.2

where γ_{lv} , γ_{sv} and γ_{sl} refer to the interfacial energies of the liquid/vapour, solid/vapour, and solid/liquid interfaces.

By means of a microsyringe a water droplet of 4 μ l is deposited on the surface. With a camera a picture of the resulting droplet is taken, that can then be analysed by computer software (SCA20).

The contact angles were measured using the drop shape analyse system DSA10 (Krüss).

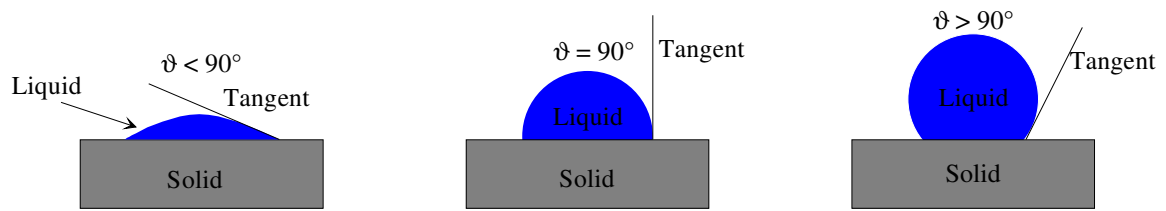


Fig 11: Schematic representation of the spreading of a water droplet on different surfaces.

As depicted in Fig 11, low values of ϑ are due to the spreading of the liquid over the surface. This indicates a very hydrophilic surface, the surface wets well. A higher value of ϑ corresponds to a hydrophobic surface. If ϑ is higher than 90° , the surface is said to be non-wetting.

G. Fluorescence recovery after photobleaching (FRAP)

FRAP is a powerful method to determine the molecular mobility and the lateral diffusion in 2-D architectures. One can obtain parameters such as the diffusion coefficient and the percentage of recovery after bleaching.

Several experimental methods have been used in the past to determine the lateral diffusion in membranes. They can be roughly classified in two categories. The first class, mostly based on bimolecular reaction, such as Heisenberg spin exchange, fluorescence quenching or neutron scattering measure diffusion over short distances. The second class, comprising FRAP, single particle tracking (SPT), nuclear magnetic resonance (NMR) or dissipation of electron spin resonance (ESR) signal gradients measures diffusion over larger distances.

In the case of tBLMs, FRAP can be used to evaluate to what extend the tether molecules influence the fluidity of the membrane.

The measurements were performed on a home-build FRAP set-up, using an Olympus IX70 microscope and an Innova 90 (Coherent) laser, as shown in Fig 12.

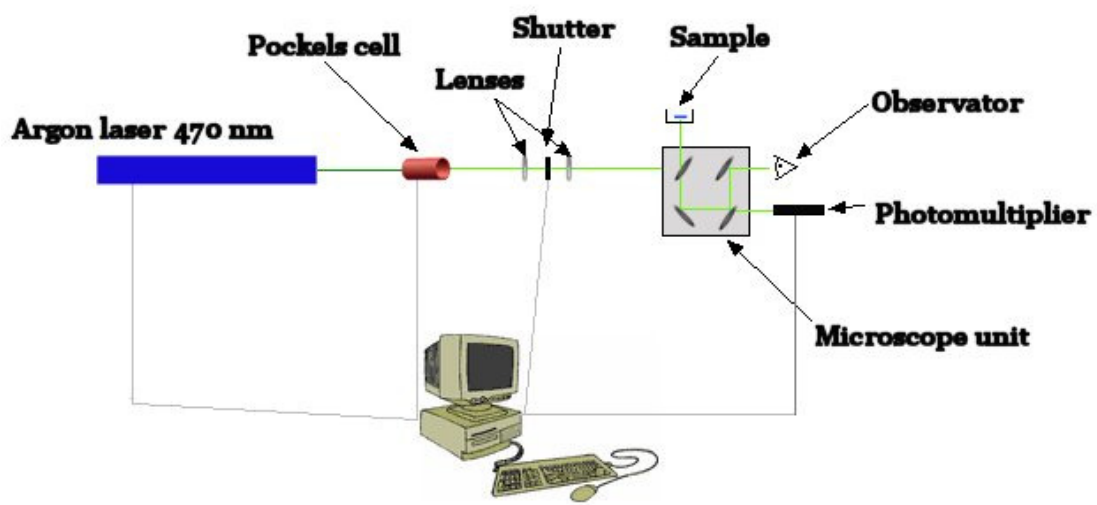


Fig 12: Scheme of the FRAP set-up.

1. Measurement procedure and evaluation:

The main steps for the FRAP method are as follows. First, a part of the membrane components is fluorescently labelled (< 0.8mol%). Their ability to be bleached irreversibly with an intense light pulse is a prerequisite for lateral diffusion measurements. Next, the sample is mounted in a water cell on top of a fluorescent microscope and an area of the membrane is focused. A small spot of the membrane (4.2μm) is irradiated with light at low intensity with an appropriate wavelength (470nm) to excite the fluorophores. The fluorescence intensity is from now on continuously registered via a photomultiplier. Thirdly, the light intensity is briefly elevated about 10⁶-fold (reaching an intensity of approx. 2W) over 100ms. This induces a rapid and irreversible photolysis of the fluorophores (more than 90% are bleached). After the bleaching period the light is attenuated to the previous level. If no lateral diffusion of the investigated membrane component takes place, the fluorescence signal evoked by the measuring beam remains constant. However, if lateral diffusion occurs, an increase of the fluorescence signal is observed due to the non-photolysed fluorophores entering into the irradiated area from the surrounding. The time dependence at the recovery of fluorescence is proportional to the lateral diffusion constant.

The following simplifying assumptions are made: the intensity being measured is so low that photolysis is negligible during the record of the fluorescence signal, and bleaching destroys the chromatophores irreversibly within a time period that is brief compared to the diffusion time. The range of diffusion constants measurable with this technique is approximately from some μm²s to 10⁶μm²s.

From the obtained recovery curve, we can fit the diffusion coefficient, using the Simplex method.

$$f(t) = F_{\infty} - [F_{\infty} - F_0] * \left\{ 1 - \exp^{\frac{-2\tau_D}{t}} * \left[I_0\left(\frac{2\tau_D}{t}\right) + I_1\left(\frac{2\tau_D}{t}\right) \right] \right\}$$

$$\tau_D = \frac{\langle r^2 \rangle}{4D}$$

Eq.3-4

where I_0 and I_1 are the Bessel functions 0. and 1. order, and τ_D the characteristic diffusion time.

Another parameter that can be calculated from the measurement is the percentage of recovery, giving a direct idea of the hindrance occasioned by the tethered molecules.

$$\text{Relative recovery} = \frac{F_\infty - F_0}{F_- - F_0} * 100\%$$

Eq.5

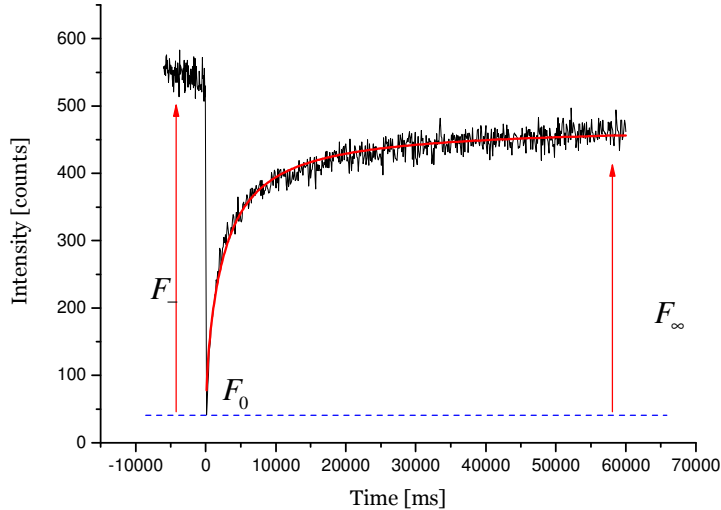


Fig 13: Typical FRAP measurement, where F_- is the fluorescence intensity before bleaching, F_0 the intensity directly after bleaching and F_∞ the recovered fluorescence; in red the fit curve.

2. Diffusion in homogeneous systems:

The lipids and lipopolymers used in our systems are in the liquid phase at room temperature. Therefore, the lateral diffusion can be explained by equations of a two-dimensional homogeneous system.

Basically, in a homogeneous, two-dimensional system the diffusion coefficient D can be defined through the relation:

$$\langle r^2 \rangle = 4Dt$$

Eq.6

where $\langle r^2 \rangle$ is the mean square displacement of a randomly moving tracer, and t is time. This mean square displacement is the second moment of the Gaussian probability distribution of displacements.

$$C(r,t) = \frac{1}{4\pi Dt} \exp\left(-\frac{r^2}{4Dt}\right)$$

Eq.7

which is the solution of the diffusion equation,

$$\frac{\partial C(r,t)}{\partial t} = D\nabla^2 C(r,t)$$

Eq.8

$C(r,t)$ is the concentration of the fluorescent material, r the spot radius, t the time and ∇^2 the Laplace operator.

Hence,

$$\langle r^2 \rangle = \int_0^\infty r^2 C(r,t) d\sigma = 4Dt$$

Eq.9

where $d\sigma = 2\pi r dr$.

Whenever the probability density $C(r,t)$ is a Gaussian distribution at long times (large distances) the diffusion coefficient is a well-defined quantity.

III. Results and discussion:

A. Langmuir Isotherms:

Isotherms of different mixtures of anchor lipid and free lipid were recorded to get insight into the self-organisation of the monolayers. All percentages are in mol%.

By spreading macromolecules at low concentration on the air/water interface, they are found to be in the so-called gas phase after solvent evaporation because of the weak interaction forces between them. Afterwards, the available spreading area is reduced, forcing them to order and so enter in the liquid phase, thus giving rise to a non-zero surface pressure. The liquid phase can be seen as a loosely packed brush conformation of the lipids due to a higher surface density, which is needed for the formation of good monolayers. By further compression (beyond π_c), the surface density in the monolayer becomes too high and a solid phase is formed.

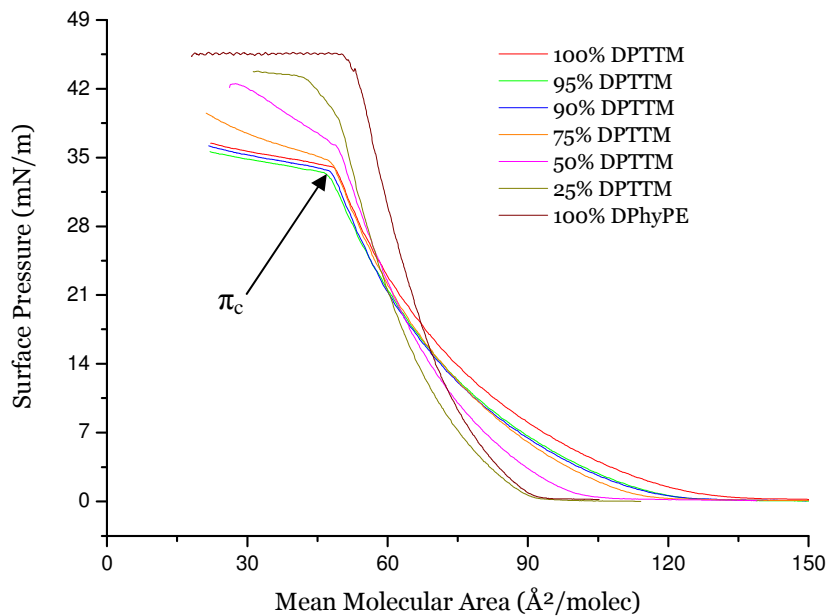


Fig 14: $\pi - A$ isotherms of the different mixtures of DPTTM and DPhyPE.

The following table summarizes the π - A values at the phase transitions.

Series	Gas-liquid transition	Liquid-solid phase transition	
	MMA ($\text{\AA}^2/\text{molec.}$)	Surface pressure π (mN/m)	MMA ($\text{\AA}^2/\text{molec.}$)
100% DPTTM	134	34	47
95% DPTTM	124	34	47
90% DPTTM	123	34	47
75% DPTTM	118	35	48
50% DPTTM	105	36	49
25% DPTTM	92	39	50
100% DPhyPE	92	45	50.5

Table 1: Phase transition in Langmuir isotherms of the mixtures.

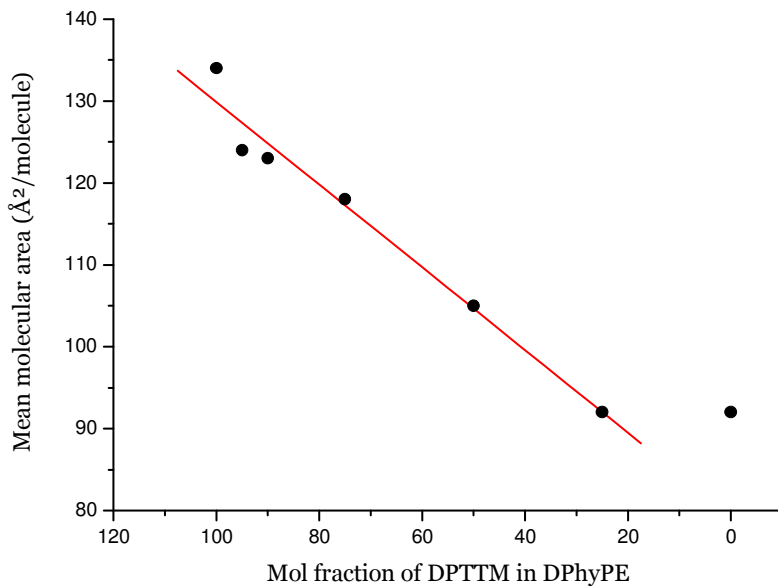


Fig 15: Decrease of the mean molecular area (MMA) at the gas-liquid phase transition as a function of the concentration of DPTTM.

Fig 15 shows a linear dependence of the mean molecular area (MMA) at the gas-liquid transition and the molecular fraction of tether lipids in the monolayer. Surprisingly, the MMA at the phase transition in the 100% DPhyPE isotherm at the transition cannot be extrapolated from the fit curve at 0% DPTTM.

Furthermore, the constant MMA value at 25% and 0% of dilution reveal that the tether lipids do not longer have an influence on the molecular organization of the DPhyPE monolayer at the gas/liquid phase transition.

This gas-liquid phase transition represents the ordering of the molecules at the air-water interface due to the reduction of the available area between the barriers. As a result of this ordering, an increase in the surface pressure π can be monitored, coming from the arising of repulsive forces between the lipids.

The differences in the chemical structures of the tether and free lipids are mainly due to the hydrophilic part. The hydrophobic tails, the two phytanoyl chains, being the same, no variation in their interaction should be noticed over the whole dilution range. The hydrophilic heads, constituted on one side of a phosphate group and on the other of an oligo(ethylene glycol) chain are therefore the sites of these rising repulsive interactions.

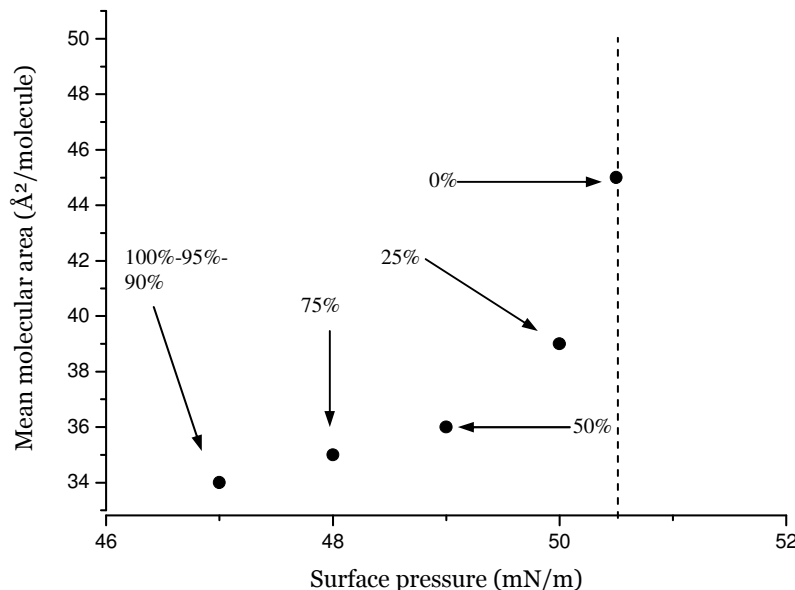


Fig 16: Exponential increase of the surface pressure-MMA ratio at the liquid-solid phase transition (at π_c); indicated is the percentage of DPTTM in the monolayer.

The next interesting point highlighted by the isotherms is the exponential increase of the MMA – Surface pressure ratio at the liquid/solid phase transition, as shown in Fig 16.

The solid phase is mainly characterized by the complete orientation of the hydrophobic chains perpendicular to the surface. An all-trans state is thus conducive to this necessary closest packing of an assembly of chains. Per contra the liquid state results from trans-gauche rotations of the chains, being therefore not coplanar; the chains are “bent” and take up a larger monolayer area [27].

The DPhyPE molecules require more energy, visualized in form of surface pressure, to undergo the configuration change, with a bigger need in space than the DPTTM molecules. Furthermore, the transition from one extreme to the other of the dilution scale follows an exponential curve. This indicates the presence of secondary effects, possibly rising from the hydrophilic parts, which should be investigated more precisely in the future.

Besides, Pallas and Pethica [28] have shown that nonhorizontal slopes in the isotherms above π_c are the result of surface-active impurities in the film.

In the isotherms presented above, the slope of the 100% DPhyPE curve is nearly perfectly horizontal and the 100%-95%-90% DPTTM curves are tending to it. These are arguments for the high purity of the products.

Now, the most astonishing is to see that with increasing mixture ratio above 10% of dilution, the slopes are becoming steeper. That shows that the repulsion forces between the molecules rise faster within the same reduction of space. This is again an indication for the disturbing action of the DPhyPE in the construction of packed DPTTM layers at higher dilution.

B. Optical fluorescence microscopy:

Using the optical microscope of the FRAP set-up, the samples can be visualized. After deposition and fixation of the fluorescent monolayer on the SiO_x support they can be observed under a 150x magnification.

Phase separations in the monolayer can be observed for different methods, as a result of different dye solubility, fluorescence quantum yield or molecular density of coexisting phases [29].

As an example, Fig 17 presents a series of textures observed under the fluorescent microscope.

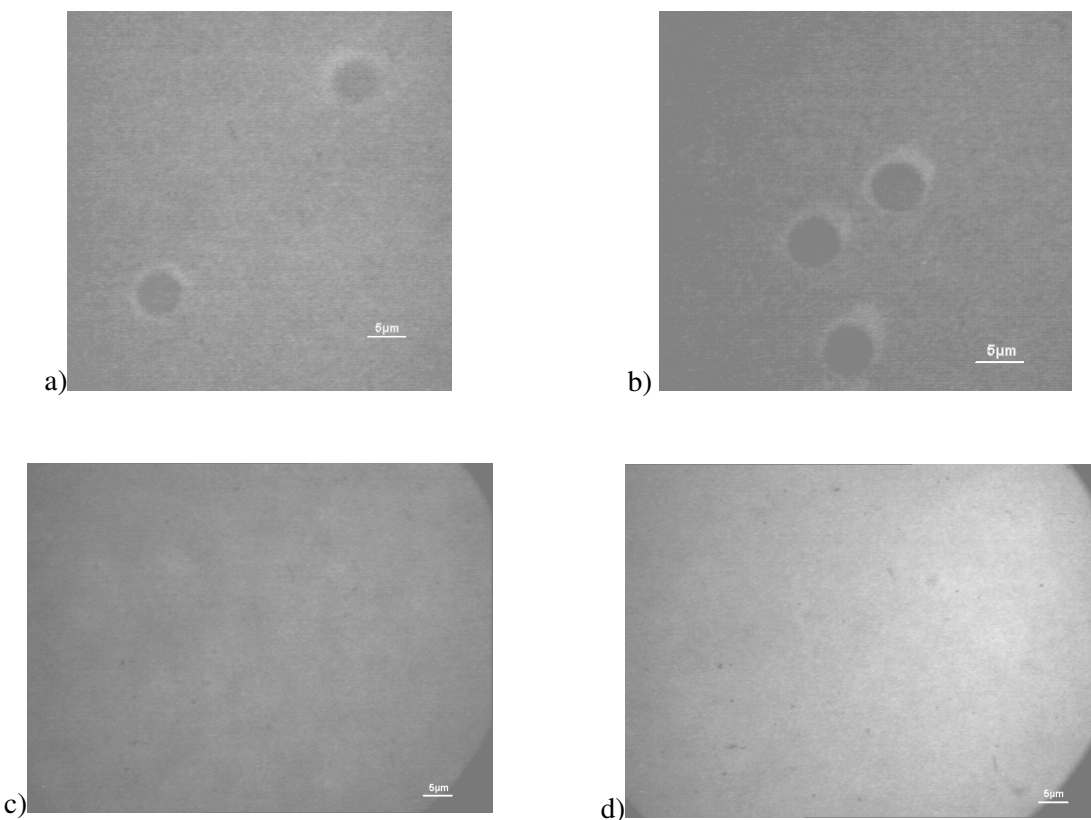


Fig 17: Fluorescence micrograph of DPTTM/DPhyPE/NBD-PE monolayers ((a) and (c) 95% DPTTM, (b) and (d) 90% DPTTM).

The micrographs a) and b) show the existence of different coexisting phases inside the membrane layer. Although the film transfers were realized under π_c , i.e. at 30mN/m, where

normally no solid phase is expected, these structures were observed on some samples prepared in the early phase of the study.

These irregularities of density in the produced film can be either explained by a qualitatively low preparation method, problems of mixing, cross-linking of the products or self-segregative behaviour of one of the components.

Optimised preparation methods, i.e. with freshly prepared and well-mixed samples, allowed the formation of homogeneous layers over large areas ($>50\mu\text{m}$), as it can be seen on the images c) and d).

C. DPTTE or DPTTM? :

The two tether molecules were successively used to determine the influence of the silane end-groups on the membrane quality.

Monolayers were produced as described before, i.e. the lipopolymer/lipid solutions in chloroform (2mg/ml) were spread at the air-water interface of an LBK-trough. 20min were allowed for the solvent to evaporate. Afterwards each monolayer was compressed to 30mN/m with a constant compression speed of 10mm/min. Once the desired surface pressure was reached, the substrates were withdrawn from the subphase at a constant rate of 7mm/min.

A qualitative analysis of the obtained monolayer was performed by contact angle measurements.

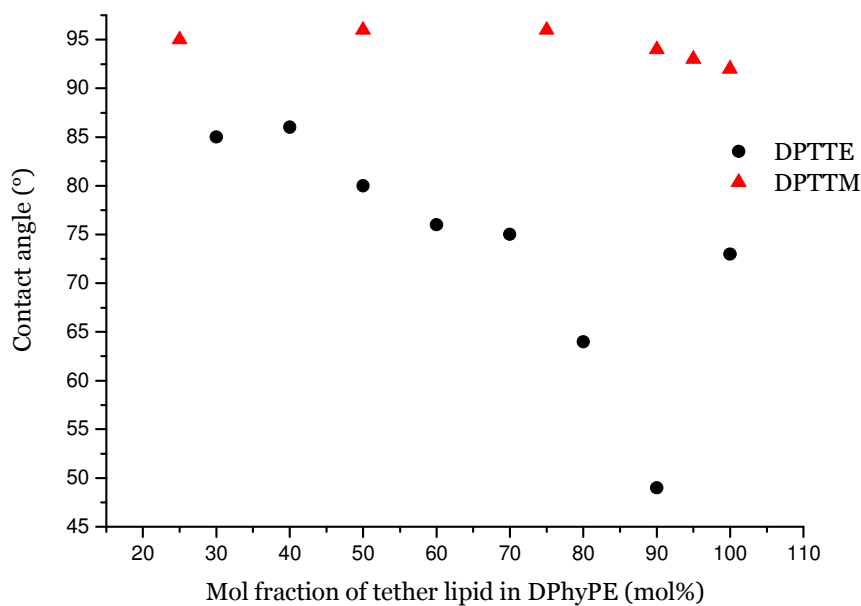


Fig 18: Measured contact angle as function of the molecular fraction of tether lipid in DPhyPE.

The first experiments were performed on DPTTE based monolayers. Contact angle measurements show that below 50mol% of dilution the monolayers were not hydrophobic enough to allow for vesicle fusion. For our system, only contact angles above 85° give a high probability for vesicle fusion to occur. Moreover, a decrease of the contact angle with

increasing DPTTE concentration could also be observed, with exception of the 100% DPTTE monolayer.

Per contra, the DPTTM monolayer had constant contact angles of approx. 90° over the whole concentration range.

This difference in the quality of the monolayers can only be induced through the unique variable of the system: the anchor group. According to the functional groups present, the grafting of the tether lipids on the support is supposed to follow a condensation reaction scheme.

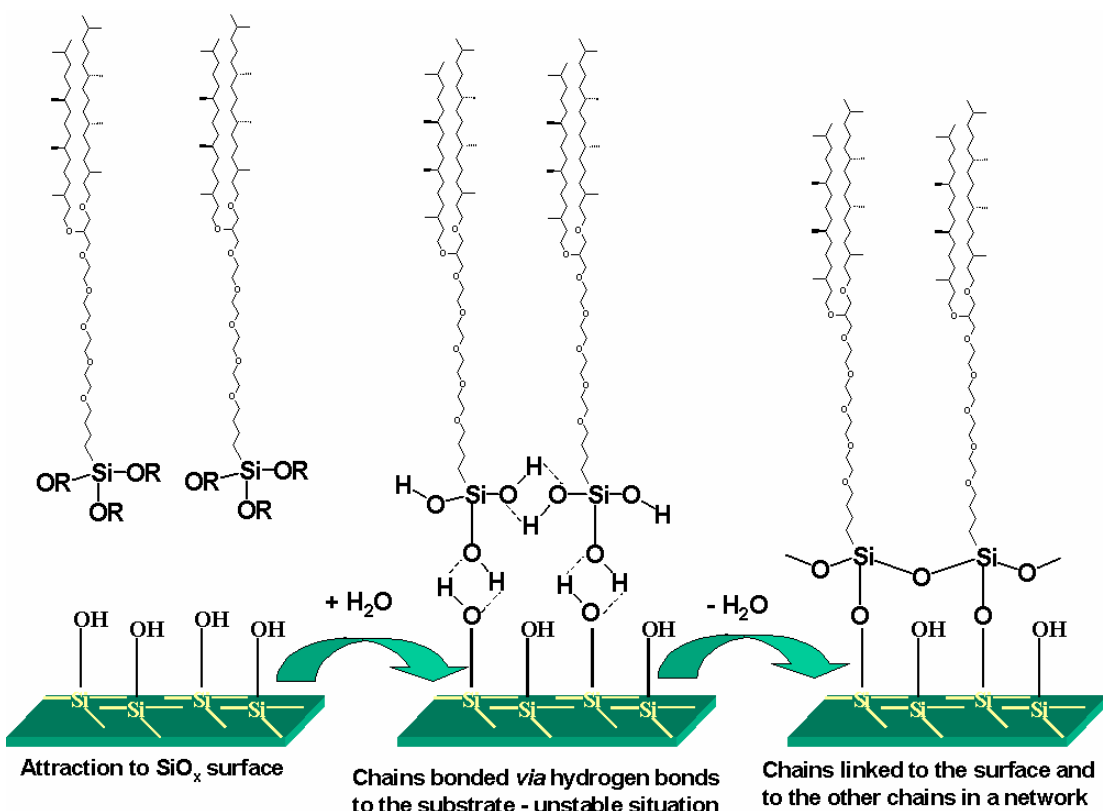


Fig 19: Condensation reaction of the tether lipids on the SiO_x surface.

As depicted in Fig 19, the first step in the condensation reaction is the hydrolysis of the $\text{Si}-\text{OR}$ groups in presence of water molecules. This occurs when the lipids are spread on the water surface of the LBK-trough.

The main differences between the two spacer molecules are the alkoxy-groups attached on the silicon; in one case ethoxy and in the other methoxy. Even if both end groups hydrolyse spontaneously in presence of water, the kinetics of these reactions are different: methoxy groups are less stable and therefore hydrolyse faster and easier than the ethoxy groups.

Thus, differences in the ability to hydrolyse and furthermore to graft properly on the substrate can partially explain the different contact angles of the DPTTE and DPTTM monolayer. However, this does not explain the decreasing angle with increasing DPTTE concentration in the monolayer, even more if the 100% DPTTE monolayer does not follow the tendency. Further investigations will be needed to explain the different grafting behaviour of the two molecules.

For the determination of the diffusion coefficient by FRAP, membranes based on DPTTM were used.

D. FRAP Measurements:

The diffusion measurements were performed in two successive series.

First, fluorescent monolayers were produced via LBK transfer on the SiO_x substrates. Thus, the diffusion coefficients for movements in the inner leaflet could be obtained. Second, always using LBK transfer, non-fluorescent monolayers were made which were covered with a fluorescent outer leaflet. This was achieved by fusion of vesicles prepared from mixtures of DPhyPE and NBD-PE (0.8mol%), and permits the separate determination of the diffusion coefficients of the outer leaflet.

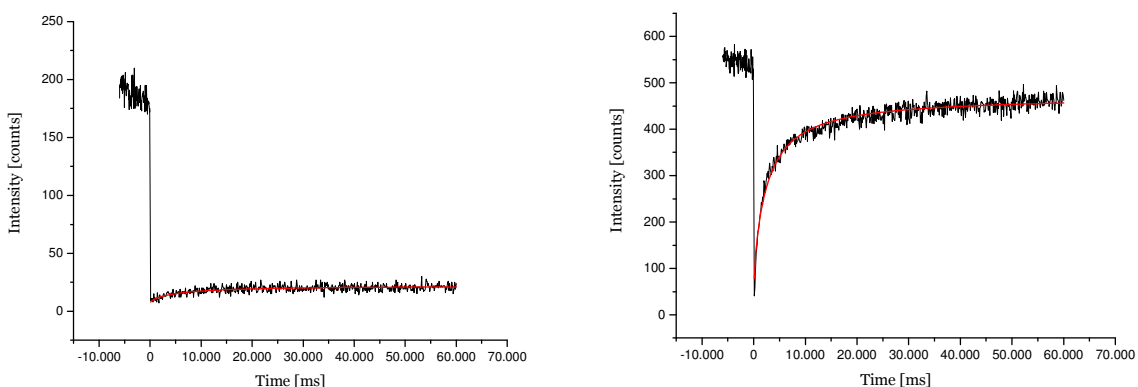


Fig 20-21: Respectively inner and outer leaflet FRAP measurements with fit curve.

1. Inner leaflet:

As described previously, the inner leaflet of the membrane has been fluorescent labelled. On each monolayer, 15 measurements were performed on various points. The same membrane composition was tested at least 3 times in order to prove the reproducibility of the results.

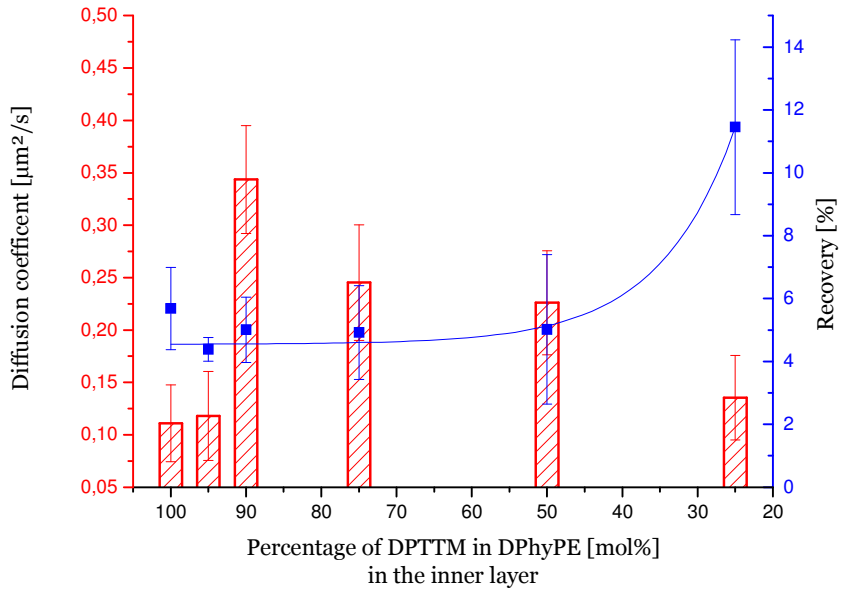


Fig 22: **Diffusion coefficient** and **recovery** of the inner layer.

The average diffusion coefficient of the inner leaflet is around $0.2\mu\text{m}^2.\text{s}^{-1}$. In literature, free floating bilayers on glass substrates show diffusion coefficients going from 1 to $2\mu\text{m}^2.\text{s}^{-1}$ [11, 30].

Here the importance of the tether lipids on the diffusion can be directly seen. The diffusion coefficient is approximatively reduced by one order of magnitude, due to the tethering of the layer.

From a more precise look at the graph, it turns out that the 100% DPTTM and 95% DPTTM monolayers exhibit diffusion coefficients around $0.1\mu\text{m}^2.\text{s}^{-1}$, although membranes without any diffusion were expected. It can be explained from the fact that the monolayers were not compressed to their solid phase, leaving some free space left between the lipids resulting in a freedom of movement, leading furthermore to these diffusions.

Second striking aspect of the graph, is the peak in diffusion at 90% DPTTM. It was assumed that the less tether lipids are present, the higher the fluidity should be.

This phenomenon could be explained by two arguments:

By decreasing the concentration of the lipopolymers in the monolayer, the latter would not be effectively supported anymore, introducing a buckling of the lipid platform, therefore allowing less diffusion.

The second argument would be based upon the observations made from the Langmuir isotherms. Over 10% dilution of the membrane with DPhyPE, the isotherm slopes indicate

“non-cooperative” interactions of both components, leading them to act as membrane impurities for each other. The more dilute the tethered membrane was, the more the slope of the curve after π_c increased. These observations would match with the constant decrease of the diffusion coefficient between 90% and 25%.

The fluorescence recovery of the membrane shows the expected behaviour, i.e. the more dilute the tethered membrane is, the more fluid lipids are embedded and therefore the recovery is higher.

2. Outer leaflet:

Similar as for the inner leaflet, 15 measurements were performed on various spots of the membrane and each membrane composition was measured at least 3 times.

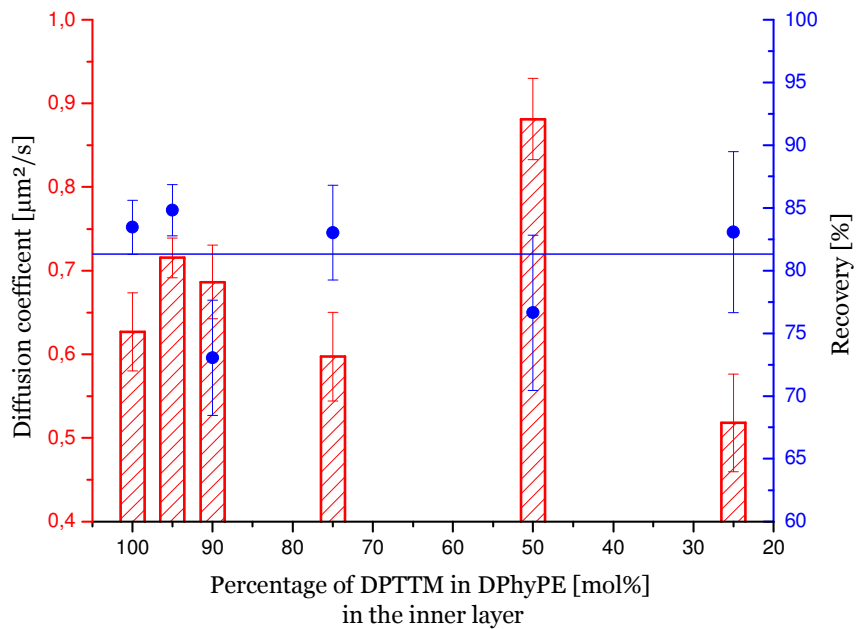


Fig 23: **Diffusion coefficient** and **recovery** of the outer layer.

The outer leaflet showed rather constant diffusion coefficients over the whole concentration range, with a small decrease at high dilutions. The average diffusion constant of $0.7 \mu\text{m}^2/\text{s}$ indicates a high fluidity of the membrane even at high tethering concentration. The constancy in diffusion shows only a small interaction effect between the inner leaflet and the outer leaflet.

The recovery rate remains constant over the concentration range at about 85%, probably due to steric hindrance at the side chains of phytanoyl groups.

Recently similar experiments have been reported on an other type of polymer-tethered membranes [31], where a dramatic decrease of the diffusion coefficient in membranes containing over 20% of tethering units were observed; over 40% of tethering, the diffusion coefficient dropped down to $0.03\mu\text{m}^2/\text{s}$. We did not observe such an effect in our system, which means, that our membranes remain fluid over the whole concentration range.

IV. Conclusion:

This report presented the results of the different measurements obtained through the study of the implication of the tethered molecules on the diffusion behaviour inside both membrane leaflets of a tBLM system.

The behaviour of the different type of lipids inside a monolayer was first studied by the Langmuir Film Balance technique. Once the properties of the lipids at the air/water interface were known, the Langmuir-Blodgett-Kuhn technique was used to transfer the created film to the silicon substrate. The quality of the obtained layer was examined by means of contact angle measurements and fluorescence microscopy. Finally, lateral diffusion inside the leaflet was measured by Fluorescence Recovery After Photobleaching.

Using the Langmuir balance technique, isotherms of the different mixtures were obtained. These highlighted a strong head to head interaction of the lipopolymers with the lipids in the gas phase up to 75% of lipid dilution. Moreover, another lipid ratio-dependent phenomena could be seen at the liquid to solid phase transition, which should be investigated in more detail.

But the main information retains the continuous changes of the properties over the whole dilution range, which is a sign of homogeneous mixing of both components and therefore prerequisite for building a good membrane.

The coated substrate, resulting from the transfer of the previously studied monolayer on a silicon wafer, enabled the investigation of the membrane quality with contact angle measurement and fluorescence microscopy. The obtained results were used as source of information for further improvements of the preparation procedure and to confirm the effect of these improvements.

The preparation of membranes showing contact angles over 90° indicates the hydrophobic nature of the proximal leaflet. These membranes had no visible domain separation under fluorescence microscope over 50 μ m ranges.

The diffusion coefficients obtained by FRAP measurements, 0.2 μ m²/s for the proximal leaflet and 0.7 μ m²/s for the distal leaflet in average, reveal the fluid behaviour of the membrane. Moreover the relative independence of the values over the dilution range makes these membranes especially interesting.

These are very positive and encouraging results for the aim that has been fixed, namely the creation of a lipid platform for biosensing applications and protein studies.

V. Literature:

1. Sackmann, E., *Physical Basis of Self-Organization and Function of Membranes: Physics of Vesicles*. Handbook of Biological Physics, ed. E.S. B.V. Vol. 1. 1995. 213-305.
2. Mueller, P., et al., *Reconstitution of Cell Membrane Structure in Vitro and Its Transformation into an Excitable System*. Nature, 1962. **194**(4832): p. 979-&.
3. Mueller, P. and D.O. Rudin, *Action Potentials Induced in Biomolecular Lipid Membranes*. Nature, 1968. **217**(5130): p. 713-&.
4. Sackmann, E., *Supported membranes: Scientific and practical applications*. Science, 1996. **271**(5245): p. 43-48.
5. Kastl, K., et al., *Kinetics and thermodynamics of annexin A1 binding to solid-supported membranes: A QCM study*. Biochemistry, 2002. **41**(31): p. 10087-10094.
6. Raguse, B., et al., *Tethered lipid bilayer membranes: Formation and ionic reservoir characterization*. Langmuir, 1998. **14**(3): p. 648-659.
7. Naumann, R., et al., *Tethered lipid Bilayers on ultraflat gold surfaces*. Langmuir, 2003. **19**(13): p. 5435-5443.
8. Schiller, S.M., et al., *Archaea analogue thiolipids for tethered bilayer lipid membranes on ultrasmooth gold surfaces*. Angewandte Chemie-International Edition, 2003. **42**(2): p. 208-+.
9. Braach-Maksvytis, V. and B. Raguse, *Highly impermeable "soft" self-assembled monolayers*. Journal of the American Chemical Society, 2000. **122**(39): p. 9544-9545.
10. Atanasov, V., et al., *Membrane on a chip: A functional tethered lipid bilayer membrane on silicon oxide surfaces*. Biophysical Journal, 2005. **89**(3): p. 1780-1788.
11. Wagner, M.L. and L.K. Tamm, *Tethered polymer-supported planar lipid bilayers for reconstitution of integral membrane proteins: Silane-polyethyleneglycol-lipid as a cushion and covalent linker*. Biophysical Journal, 2000. **79**(3): p. 1400-1414.
12. Woese, C.R. and G.E. Fox, *Phylogenetic Structure of Prokaryotic Domain - Primary Kingdoms*. Proceedings of the National Academy of Sciences of the United States of America, 1977. **74**(11): p. 5088-5090.
13. Shimshic.Ej and McConnel.Hm, *Lateral Phase Separation in Phospholipid Membranes*. Biochemistry, 1973. **12**(12): p. 2351-2360.
14. Hsieh, C.H., et al., *Membrane packing geometry of diphytanoylphosphatidylcholine is highly sensitive to hydration: Phospholipid polymorphism induced by molecular rearrangement in the headgroup region*. Biophysical Journal, 1997. **73**(2): p. 870-877.
15. Yamauchi, K., et al., *Archaeabacterial Lipids - Highly Proton-Impermeable Membranes from 1,2-Diphytanoyl-Sn-Glycero-3-Phosphocholine*. Biochimica Et Biophysica Acta, 1993. **1146**(2): p. 178-182.
16. Mingins, J., D. Stigter, and K.A. Dill, *Phospholipid Interactions in Model Membrane Systems .1. Experiments on Monolayers*. Biophysical Journal, 1992. **61**(6): p. 1603-1615.
17. Stigter, D., J. Mingins, and K.A. Dill, *Phospholipid Interactions in Model Membrane Systems .2. Theory*. Biophysical Journal, 1992. **61**(6): p. 1616-1629.
18. Lindsey, H., N.O. Petersen, and S.I. Chan, *Physicochemical Characterization of 1,2-Diphytanoyl-Sn-Glycero-3-Phosphocholine in Model Membrane Systems*. Biochimica Et Biophysica Acta, 1979. **555**(1): p. 147-167.
19. Kuhn, H. and D. Mobius, *Systems of Monomolecular Layers - Assembling and Physico-Chemical Behavior*. Angewandte Chemie-International Edition, 1971. **10**(9): p. 620-&.

20. Langmuir, I., *Pilgrim trust lecture - Molecular layers*. Proceedings of the Royal Society of London Series a-Mathematical and Physical Sciences, 1939. **170**(A940): p. 0001-0039.
21. Blodgett, K.B., *Films built by depositing successive monomolecular layers on a solid surface*. Journal of the American Chemical Society, 1935. **57**(1): p. 1007-1022.
22. Blodgett, K.B., *Monomolecular films of fatty acids on glass*. Journal of the American Chemical Society, 1934. **56**: p. 495-495.
23. Ostwald, W., *On the theory of flotation*. Kolloid-Zeitschrift, 1932. **58**(2): p. 179-183.
24. Langmuir, I., *The constitution and fundamental properties of solids and liquids. II. Liquids*. Journal of the American Chemical Society, 1917. **39**: p. 1848-1906.
25. Möhwald, H., *Phospholipid Monolayers*. Handbook of Biological Physics, ed. E.S. B.V. Vol. 1. 1995. 161-211.
26. Kalb, E., S. Frey, and L.K. Tamm, *Formation of Supported Planar Bilayers By Fusion of Vesicles to Supported Phospholipid Monolayers*. Biochimica Et Biophysica Acta, 1992. **1103**(2): p. 307-316.
27. Bell, G.M., L.L. Combs, and L.J. Dunne, *Theory of Cooperative Phenomena in Lipid Systems*. Chemical Reviews, 1981. **81**(1): p. 15-48.
28. Pallas, N.R. and B.A. Pethica, *Liquid-Expanded to Liquid-Condensed Transitions in Lipid Monolayers at the Air Water Interface*. Langmuir, 1985. **1**(4): p. 509-513.
29. Weis, R.M. and H.M. McConnell, *Two-Dimensional Chiral Crystals of Phospholipid*. Nature, 1984. **310**(5972): p. 47-49.
30. Tamm, L.K., *Lateral Diffusion and Fluorescence Microscope Studies On a Monoclonal-Antibody Specifically Bound to Supported Phospholipid-Bilayers*. Biochemistry, 1988. **27**(5): p. 1450-1457.
31. Deverall, M.A., et al., *Membrane lateral mobility obstructed by polymer-tethered lipids studied at the single molecule level*. Biophysical Journal, 2005. **88**(3): p. 1875-1886.

Acknowledgments:

I first want to thank Dr. Ingo Köper and Prof. Dr. Wolfgang Knoll for giving me the possibility to do my Master Thesis on this very interesting subject in this remarkable institute.

Thanks also to Prof. Dr. Pietzsch for supervising my work at the Martin-Luther University Halle-Wittenberg.

I especially want to acknowledge all the members of the group: Catherine, Inga, Petia and Vladimir, who helped me to step into this new field.

Finally, thanks to all Knollies for creating this extraordinary atmosphere in- and outside the institute.